DOI 10.1515/aot-2013-0027 — Adv. Opt. Techn. 2013; 2(4): 291–300

Tutorial

Julius Muschaweck and Christopher Wiesmann*

Extracting light out of LEDs

Abstract: 'External quantum efficiency', that is, the number of photons generated per electron passing through the p-n junction of an LED is probably the most important number to quantify the performance of an LED chip. Although advances in epitaxy have increased the fraction of radiative recombination to extremely high values, the extraction of the precious photons that are trapped in a high refractive index crystal is still tricky. In this brief tutorial, we look at the physics of light extraction both from a geometrical optics/thermodynamic and a wave optics point of view, discussing both random and deterministic surface structures.

Keywords: LED; light extraction; nonimaging optics; photonic crystal.

OCIS codes: 220.2945; 220.4298; 080.2175; 080.2740; 080.4298; 250.0250.

***Corresponding author: Christopher Wiesmann,** OSRAM GmbH, Werner-von-Siemens-Str. 6, 86159 Augsburg, Germany, e-mail: c.wiesmann@osram.com
Julius Muschaweck: OSRAM GmbH, Werner-von-Siemens-Str. 6, 86159 Augsburg, Germany

1 Introduction

Currently, two material systems dominate the LED industry: InGaAlP for the long wavelength part of the visible spectrum (red/yellow), and InGaN for the shorter wavelengths (blue/green). Extremely thin multi-quantum wells and heterostructures are commonly used to convert electron-hole pairs to photons with high internal quantum efficiency [1]. However, the refractive index of the crystal embedding the quantum wells ranges from approximately $n\approx2.4$ for the InGaN LEDs up to $n\approx3.5$ for InGaAlP, values much higher than those for air ($n\approx1.0$) or commonly used silicone encapsulation compounds ($n\approx1.4$). Therefore, if the LED surfaces were specular, as they used to be in the early days, much of the generated light would be totally internally reflected instead of being refracted out of the LED crystal.

Over the years, the LED industry has learned to avoid photon loss mechanisms inside the LED chips. Absorbing substrates have been replaced by transparent substrates, and silver mirrors have been placed on the back side of thin film chips, to give the totally internally reflected photons another chance to escape.

However, it is not immediately clear how structuring the chip surface affects the way light is coupled out of LEDs. To what extent is it possible to avoid trapping of light by randomly roughening the surface, or by applying deterministic structures, for example, photonic crystals? In this tutorial, we present answers to these questions derived from first principles, namely thermodynamics and Maxwell's equations.

2 Geometrical optics viewpoint

We use the thin film LED geometry shown in Figure 1 to consider the dominant paths of light in the geometrical optics approximation, that is, neglecting diffraction and coherence. Rays are generated in the p-n junction. Some of them are refracted out from the semiconductor material, with a high refractive index of $n\approx2.4$ for the blue/green emitting InGaN material system, or $n\approx3.5$ for the red/yellow emitting InGaAlP material system, into the embedding air ($n\approx1$) or silicone ($n\approx1.4$). Other rays are reflected back into the LED chip, where they are either absorbed in the junction or where they pass through the junction towards the back side of the chip. At present, we are not interested in what happens to the reflected rays, or to rays emitted downwards in the first place. Instead, we focus our attention on the primary interaction of a ray with the chip surface.

It is indeed possible to perfectly extract guided light from a high index solid [2]. A structure as proposed in this reference is shown in Figure 2. Can we hope to achieve similar results for the whole LED surface when we cover it with a 'forest' of such pyramidal structures? The answer is a clear 'no'.

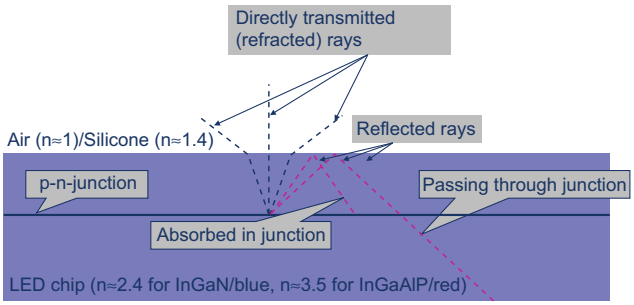

Figure 1 Structure of a thin film LED chip with the dominant light paths. Drawing is not to scale: in reality, the structure is much thinner compared to its width.

Microscopically, many of the rays shown in Figure 2, especially those emitted from the bottom of the pyramid, will intersect adjacent pyramids which bend them back into the LED. Macroscopically, however, it turns out that such an out-coupling structure would violate the Second Law of Thermodynamics.

To see why, we conduct a Gedankenexperiment (thought experiment). First, we note that with a slightly tapered cone of a fully transparent material with a sufficiently high refractive index, as shown in Figure 3, we can concentrate diffuse light coming from air onto a smaller area within the material, using only total internal reflection.

Second, we assume that we place such an ideal hypothetical out-coupling structure onto the smaller cap of such a cone – if we had such a structure, it does not have to be on an LED, we can put it anywhere we want for our purposes. If this were possible, we could cascade such devices, to concentrate the light entering the large surface from air onto a surface that is smaller by a factor of, say, 32, and entirely extract it from that surface into air, again. Assuming ideal antireflective coatings, the process would be 100% efficient.

Third, we place a blackbody radiator with a temperature of, say, T_{cold}=300 K next to the larger entrance surface,

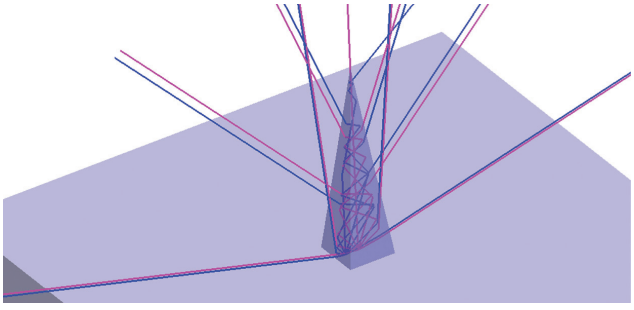

Figure 2 Ray tracing image of a single pyramid on a GaN chip surface.

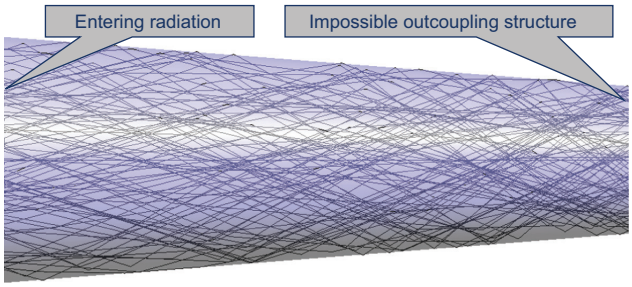

Figure 3 When diffuse radiation coming from air enters the left surface of a slightly tapered cone from all directions, the rays are refracted into the material due to higher refractive index of the cone compared to air. Because their angle with the optical axis is less than the total internal reflection angle, all of them are guided by total internal reflection to the right side, where they would be entirely extracted by a hypothetical ideal out-coupling structure.

and another blackbody radiator with, say, T_{hot}=600 K next to the final, small exit surface. The blackbody radiators emit thermal radiant flux Φ according to the Stefan-Boltzmann Law,[1]

$$\Phi = A n^2 \sigma T_{cold}^4 \quad (1)$$

where A, n, σ, T denote emission area, refractive index, the Stefan-Boltzmann constant and the absolute temperature, respectively.

The Gedankenexperiment and its energy balance are shown in Figure 4. Radiative heat would flow from T_{cold} to T_{hot} and back according to Eq. (1). The arrangement of temperatures and areas would cause a spontaneous net flow of heat from the colder to the hotter thermal reservoir, which is forbidden by the Second Law. If such devices were possible, we could send this net flow of heat into an engine and generate, for example, electricity, from ambient heat alone.

This reasoning is essentially derived from the insight that radiation is associated with entropy as soon as the photons are distributed over more than a single mode.

Having shown that complete direct extraction of radiation from an LED chip is not possible, the obvious next question is: What fraction of radiation can be extracted directly by micro-structuring the LED surface, taking into account that the radiance emitted by a p-n junction generally varies over location and direction, unlike blackbody radiation.

1 Note the factor of n^2, which is required by the theory, but often erroneously omitted. Within a cavity of given volume and homogeneous wall temperature, the radiative energy scales with n^3, because there is more room for modes with shorter wavelength, and therefore the density per area must scale with n^2.

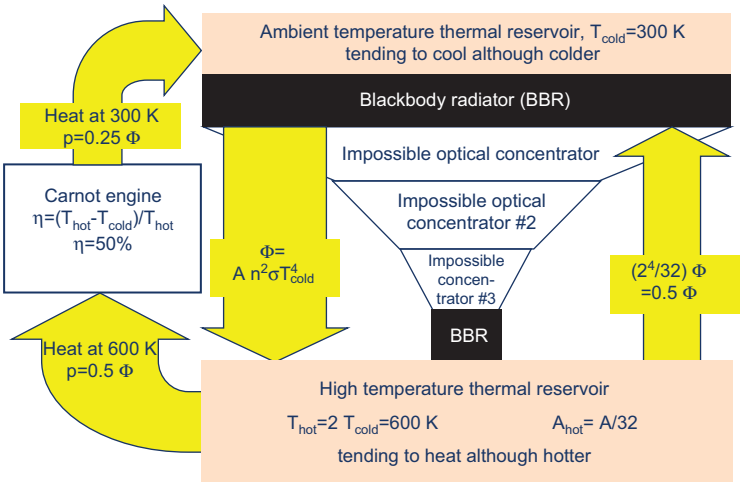

Figure 4 Gedankenexperiment showing that surface treatments with full light extraction from an LED violate the Second Law.

We assume that no absorption and emission of photons near the visible range occurs in the surface structure, that is, the surface structure is a passive system.

To such systems we can apply the theory of nonimaging optics [3]. Following the standard procedure in nonimaging optics, we may place so-called reference surfaces into the light path at our discretion, to analyze the properties of the ray bundle as it passes through the reference surfaces we chose. As shown in Figure 5, we choose two reference surfaces: an inner reference surface S_i just inside the chip, and an outer reference surface S_o just outside the chip. Thus, S_i is embedded in a material of high refractive index n_i, whereas S_o is embedded in a material of low refractive index n_o.

We describe the direction of each ray as it passes through a reference surface by its wave vector $\mathbf{k}$, with the vacuum wavelength λ_0 as unit of length. Thus, $|\mathbf{k}|=1$ in vacuum or air, and $|\mathbf{k}|=n$ in a medium with refractive index n. Also, we restrict our attention to rays leaving S_i and S_o upwards, that is, to the direct light extraction path we wish to analyze.

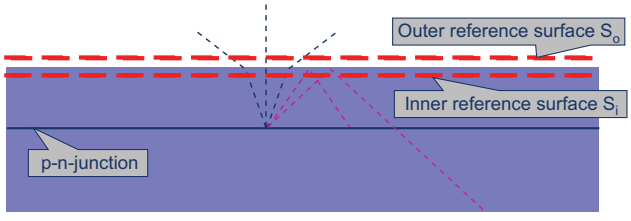

Figure 5 Placement of reference surfaces in the thin film LED chip. The lower reference surface is located just inside the chip, the upper reference surface is located just outside.

We introduce a three-dimensional (3D) Cartesian coordinate system such that the x and y axes are parallel to the planar surfaces S_i and S_o, whereas the z axis points upward. Then, $\mathbf{k}=(k_x, k_y, k_z)$ is entirely determined by its tangent components k_x and k_y because the length of $\mathbf{k}$ is known (there is no ambiguity regarding the sign of k_z because $\mathbf{k}$ points upwards). In Figure 6, it is shown how this description leads to an intuitive description of Snell's Law as an aspect of a Conservation Law.

As a ray intersects the reference surfaces S_i or S_o, the location of the intersection point can be unambiguously described by its x and y components (the z component in this case is a constant describing the vertical shift of the surface). Thus, a ray intersecting a given reference surface is given by four numbers: (x, y, k_x, k_y). These four numbers, which depend continuously on the location and direction of the corresponding ray, span a four-dimensional (4D) space $\boldsymbol{P}$, the phase space of geometrical optics. It is at first challenging, but very fruitful, to simultaneously view a ray as an extended half-line in 'real' 3D space, and as a simple point in 4D phase space.[2]

As a note, this description can be extended in a natural way to non-planar reference surfaces, by viewing a curved surface as a two-dimensional (2D), differentiable manifold M with a suitable chart

$$\varphi:\mathbf{R}^2 \supset U \mapsto \mathbf{R}^3;\ (u, v) \to p=(x, y, z).$$

2 To 'simultaneously view' means to have a bijection, mathematically speaking. If we have two seemingly unrelated sets and a bijection between these sets, then every theorem that applies to the first set is true for the second set, and *vice versa* – an extremely powerful tool to gain insights that are otherwise not obvious at all.

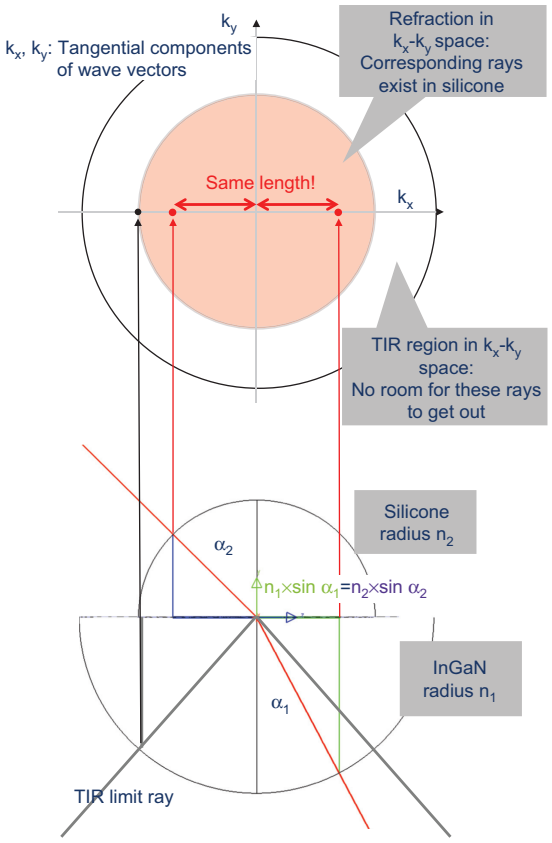

Figure 6 Refraction at specular surfaces in phase space. At the bottom, Snell's Law is revisited: by assigning the semicircles a radius proportional to the refractive index n, it becomes clear that the tangent component of the wave vector is conserved under refraction. At the top, the inner circle shows the k_x and k_y components of those rays that can exist on both sides, whereas the outer ring corresponds to total internal reflection (TIR) rays.

Let T_pM be the (2D) tangent space at p with a suitable Cartesian coordinate system, and let $t=(t_1, t_2)\in T_pM$ be a tangent vector with $|t|<n$, where n is the refractive index of the medium embedding M. Then, u, v may be used as the two location coordinates of the phase space on M, whereas t_1, t_2 play exactly the same role as the directional coordinates k_x, k_y in our simple planar case, where this more general mathematical description is not needed. For a less terse description of the phase space of geometrical optics, see [3].

A ray bundle passing through a reference surface, that is, a set of rays with finite spatial and angular extent, will then be described by a subset $\mathbf{S}\subset\mathbf{P}$ with a finite 4D volume E, which is known as the étendue of $\mathbf{S}$.

A ray bundle that passes through every point on the reference surface and from each surface point into all available directions, that is, the complete hemisphere, will fill the whole phase space. Its étendue is given simply by multiplying its spatial extent, that is, the area A of the reference surface, measured, for example, in mm^2, with its angular extent. Although it is obvious how to measure area, the correct way to measure angular extent in phase space may require some explanation. If the directional coordinates of phase space were spherical angles, we would simply use the solid angle to measure angular extent. However, it is not the spherical angles but the tangent components of the wave vector, k_x, k_y, which describe direction in phase space. Thus, an angular range of solid angle $d\Omega$ around a ray with incidence angle α covers an angular extent of $dk_x dk_y = n^2\cos\alpha\, d\Omega$ in phase space. Therefore, the appropriate measure of the angular extent of phase space is not the solid angle, but the area of the corresponding circle with radius n shown on the upper side in Figure 6, typically measured in steradiants.[3] Thus,

$$E_{phase\ space} = An^2\pi, \tag{2}$$

measured in mm^{2}sr. For example, the étendue of a 1-mm^2 reference surface within an InGaN LED chip with n=2.4 evaluates to $E\approx 18$ mm^{2}sr, whereas an equal size reference surface in silicone with n=1.41 contains only $E\approx 6.3$ mm^{2}sr. In a very real sense, there is less room for light in silicone than in InGaN.

This description of light passing through a reference surface is purely geometrical. To make the connection to the Second Law, we consider the density L of flux in phase space,

$$L = \frac{d\Phi}{dE}, \tag{3}$$

which is traditionally known as generalized radiance [3], where 'generalized' denotes here the inclusion of the factor n^2. In the remainder of this paper, we will simply use the term radiance for L.

Because the blackbody radiation spectrum is the spectral distribution of spectral radiance

$$L_\lambda = \frac{dL}{d\lambda}, \tag{4}$$

it is now easy to see that the above Gedankenexperiment, fully extracting of light from an optically denser material using surface structures, would violate the Second Law by

3 As shown in [3], the étendue of a ray bundle is invariant under free space propagation, and under refraction and reflection at smooth surfaces. It is precisely this invariance, known as the law of étendue conservation, which justifies the use of k_x, k_y as directional coordinates in phase space instead of spherical angles, which might look like a more intuitive choice.

increasing radiance in a passive optical system. The same radiant flux would be compressed into a much smaller phase space volume and would become 'hotter'.

We now have the tools at hand to quantitatively answer the question: If full direct extraction is fundamentally impossible, then what is the maximal fraction η_{max} of radiant flux that can be directly extracted? The analogy to be used is that of two vessels of fixed volume, the larger one being filled with some material, and the smaller one being empty. Clearly, we can fill the smaller vessel with the maximum amount of mass by repeatedly selecting that bit of matter from the larger vessel which has the highest density, until the smaller vessel is filled, thus making a pareto-optimal choice [4]. For radiant flux emitted from a Lambertian source, whose radiance is perfectly uniform – the vessels are filled with matter of homogeneous density – η_{max} is simply given by the étendue ratio. However, if the phase space within the denser material is filled with inhomogeneous radiance, that is, if the radiation possesses some directionality, then it is possible to extract a larger fraction of radiant flux.

What is the radiance distribution of light emitted by a p-n junction within a chip? Neglecting wave optical effects, this depends on the transparency of the junction. The junctions of red/yellow emitting InGaAlP LEDs have low transparency, absorbing most of the incident light, whereas the junctions of blue/green emitting InGaN LEDs are fairly transparent, as can be seen in Figure 7.

Viewing the junction as an agglomeration of tiny light emitting and light absorbing sites within a transparent material, for example, a gas, the radiance distribution depends on the density of these sites. If the junction is densely populated by these sites, it is not transparent, and the emission characteristic will be Lambertian, similar to that of dense white paint (surface emission). If the junction is sparsely populated, it is highly transparent, and the emission characteristic will be similar to that of a low pressure gas discharge lamp, shaped as a thin slab (volume emission). Whereas the constant radiance of a planar Lambertian source yields the familiar cos θ intensity distribution, the intensity distribution of a low density gas is isotropic, because the isotropically emitting particles hardly interact. Thus, the radiance $L(\theta)$ of a transparent InGaN p-n junction varies as $L(\theta)=L_0(\cos\theta)^{-1}$, in the geometrical optics approximation.

This radiance distribution is visualized in Figure 8.

According to [4], the maximal fraction of directly extractable flux can be computed by integrating $L(\theta)$ over the outer ring. With a little algebra,[4] this yields a maximal directly extractable flux of $\frac{n_o}{n_i}=\frac{1.41}{2.4}=59\%$, considerably more than the fraction of $\left(\frac{n_o}{n_i}\right)^2=35\%$ which we obtain for a Lambertian p-n junction, but also considerably less than the 100% we have seen to be forbidden by thermodynamics.

However, it is not easy in practice to achieve such out-coupling properties. For a perfectly smooth, specular, antireflective coated surface, the near normal rays corresponding to the inner circle in Figure 8 will be refracted out (containing only 19% of the total flux), whereas the more oblique rays will incur total internal reflection – exactly the opposite of what we would need. A roughened surface will scramble these directions, approximating the same out-coupling efficiency which we can obtain for a

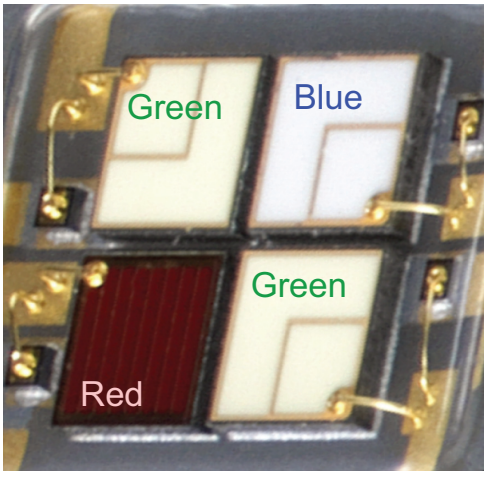

Figure 7 Close up photograph of an RGB multicolor LED package for video projection. All LED chips have a diffuse surface on top. However, the red emitting InGaAlP LED on the lower left looks dark red, showing that most of the incident light is absorbed in the junction, whereas the three other InGaN LEDs are nearly white, showing that their junctions are nearly transparent.

4 The flux ϕ in the outer ring R is obtained by integration:

$$\begin{aligned}\phi &= \int_R L\,dk_x\,dk_y = n_i^2 \int_R L\cos\theta\,d\Omega \\ &= n_i^2 \int_R L\cos\theta\sin\theta\,d\theta d\varphi \\ &= 2\pi n_i^2 L_0 \int_{\theta_{min}}^{\pi/2} \sin\theta\,d\theta \\ &= 2\pi n_i^2 L_0 \cos\theta_{min}\end{aligned}$$

whereas the flux in the whole circle is, by the same reasoning, equal to $2\pi n_i^2 L_0$. Thus, the flux fraction in the outer ring is equal to $\cos\theta_{min}$. Now, the area of the inner circle is $n_o^2\pi$. To match this area, the outer ring must have an inner radius of $\sqrt{n_i^2-n_o^2}$. Let θ_{min} be the ray angle corresponding to the inner radius of the outer ring. Then, $\sin\theta_{min}=\sqrt{n_i^2-n_o^2}/n_i$ and thus $\cos\theta_{min}=n_o/n_i$.

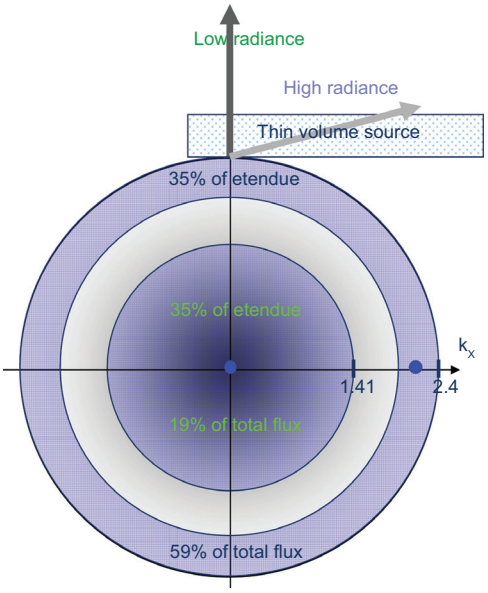

Figure 8 Radiance distribution of a thin planar volume source over **k**, where the source lies in InGaN with refractive index n_i=2.4. Dark and bright shading indicates low and high radiance, respectively. The highest radiance appears in directions nearly parallel to the surface, the lowest radiance in near normal directions. Assuming the medium is embedded in silicone (n_o=1.41), the inner circle covering a fraction of $\left(\frac{n_o}{n_i}\right)^2$=35% contains rays that would be refracted out at a specular chip surface into the embedding silicone. These rays contain only 19% of the total flux, due to their relatively low radiance. In contrast to this, the outer ring, with a width chosen to cover the same 35% of étendue, contains high radiance rays with 59% of the total flux.

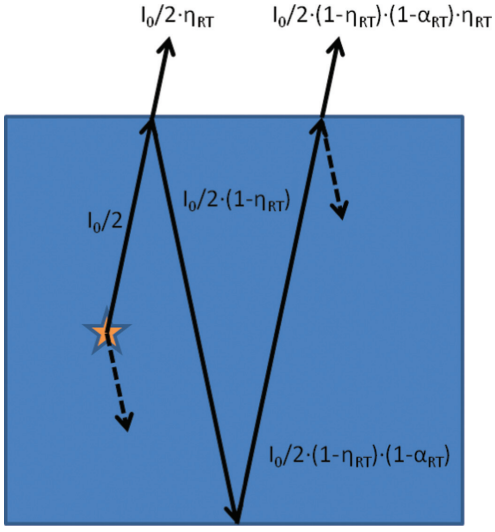

Figure 9 Sketch illustrating the round-trips of light emitted upwards from the source and propagating in an LED while undergoing losses of α_{RT} and extraction of η_{RT} per round-trip. The downwards emitted light can be treated accordingly. Summing up the extracted flux yields the overall extraction efficiency η_{extr}.

Lambertian p-n junction. Surface structures that preferably couple-out oblique rays are conceivable, but the shape of the micro-structures will have to be fairly intricate.

In practice, an additional effect not yet considered is used to couple-out a maximum fraction of the generated flux. Light that is reflected by the chip surface is not lost, but will be recycled through two main mechanisms. Part of the reflected light is absorbed and re-emitted by the junction, and another part is transmitted through the junction, back-reflected by a mirror below the junction and diffusively transmitted through and/or reflected by a scattering layer. Such light gets a second chance to be extracted. Let us assume, that the fraction η_{RT} of the internal propagating flux is extracted per round-trip, whereas the fraction α_{RT} is absorbed, as indicated in Figure 9.

Now, the total extraction efficiency is given by a geometrical series reading:

$$\eta_{extr}=\frac{0.5(2-\alpha_{RT})\eta_{RT}}{1-(1-\eta_{RT})(1-\alpha_{RT})}. \quad (5)$$

If these recycling mechanisms were 100% efficient, that is, α_{RT}=0, complete out-coupling could be achieved. This is not in contradiction to thermodynamics: it is well known that a 'gray' thermal emitter is perfectly usable to cover the walls of a cavity which will emit blackbody radiation with higher radiance.[5] Increasing radiance is possible by directing a fraction of the emitted light back to the emitter itself. This approach is taken to its extreme in a semiconductor diode laser, where nearly all the light is compressed into a very small number of modes, through stimulated emission, which is a special form of interaction of emitted light with the source itself.

This takes us to the next step in our considerations. Geometrical optics, on which this section is based, disregards not only diffraction but also coherence. However, typical LED chips often have rather small dimensions. Therefore, it seems questionable to neglect diffraction, coherence and interference. What can we learn from analyzing the LED chip with a wave optical approach? And,

5 Assume that the inner wall of a large cavity at temperature T absorbs a nonzero fraction α of the incident light and reflect the remaining light. As Kirchhoff [5] has shown in his famous 1860 paper, the ratio ε between the thermal radiation emitted by the non-black wall itself and the Planck blackbody value is exactly equal to α, even when α varies with location, direction wavelength and polarization. Light incident on a small hole in the wall of the cavity will be (nearly) completely absorbed after multiple interactions with the wall: $\alpha=\varepsilon=1$ for the hole, which is why blackbody radiation has its name, and is also called Hohlraumstrahlung (cavity radiation).

can we conceive chip architectures exploiting insights from wave optics?

3 Wave optics viewpoint

In this section, we will derive the impact of a (periodic) structuring of the LED in order to extract as much light from the structure as possible. For the wave optical viewpoint, we need to take into account the interaction between the light waves and their environment, that is, solve Maxwell's equations. For instance, in a typical thin film LED – if there are no scattering and re-absorption effects – the light distribution in k_x-k_y is strongly modulated due to its confinement between the back mirror and the semiconductor-ambient interface. According to the interferences at a given frequency light will be allowed to certain discrete k-values only. Hence, in contradiction to Figure 8, not the whole k_x-k_y-area is filled. If the structure supports two guided modes, that is, light having a total tangential wave vector component $k_{||}=\sqrt{(k_x^2+k_y^2)}>1$, those modes form circles in k_x-k_y as shown in the inset of Figure 10. Taking the frequency dependence of the total tangential wave vector component into account gives the so-called dispersion relation as depicted in Figure 10. The dashed line labeled 'light line' indicates the dispersion of the critical angle, that is, $k_0=\frac{2\pi}{\lambda_0}$, and the 'semiconductor light line' shows $k_n=\frac{n2\pi}{\lambda_0}$ with n being the refractive index of the semiconductor. All modes with $0<k_{||}<k_0$ can radiate into the ambient medium, whereas modes with $k_0<k_{||}<nk_0$ are guided and cannot escape the structure. For more details on planar LED stacks, please see [6].

To extract the guided modes their in-plane k-vector length needs to be smaller than k_0 for extraction to air. This can be achieved by introducing a periodic corrugation of the slab as shown in Figure 11 – a 2D photonic crystal. Its periodicity is depicted by reciprocal vectors **G** that form a lattice with primitive reciprocal lattice vector length $G_0\sim\frac{2\pi}{a}$ and a the lattice pitch. According to Bragg's law of diffraction, the correct choice of the reciprocal lattice vector length gives $|\boldsymbol{k}\text{-}\boldsymbol{G}|<\boldsymbol{k}_0$ and hence the high radiance parts in **k**-space are extracted.

For a hexagonal lattice as shown in the inset of Figure 11 the dispersion relation in Figure 12 is obtained for the case of a negligible refractive index contrast between the slab and the holes. This dispersion relation is generated by first superimposing the Brillouin zone as shown in the inset of Figure 12 into Figure 11. Secondly, when increasing the frequency the in-plane k-vector of the guided modes increases, also according to Figure 10. By following the intersections of the mode circles with the edges of the Brillouin zone, the dispersion relation builds up, that is, it is a representation of Bragg's law of diffraction.

Especially above reduced frequencies of $u>0.65$ all guided modes can be diffracted to air by some superposition of the reciprocal lattice vectors $\mathbf{G}_1$ and $\mathbf{G}_2$ as the Brillouin zone is completely enclosed by a circle with radius k_0. In a very familiar manner, a randomly textured surface also extracts every part of every mode partially due to the huge number of reciprocal lattice vectors **G** that

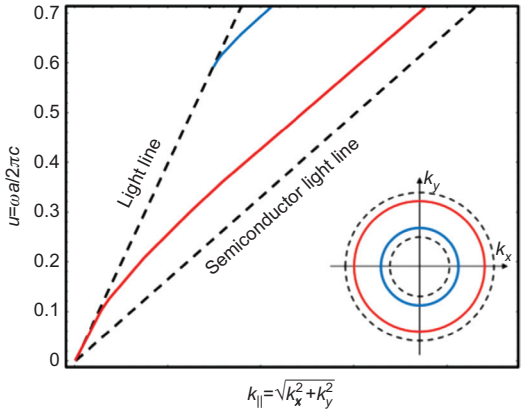

Figure 10 Dispersion relation of an uncorrugated semiconductor slab in air supporting two guided modes (red and blue). The inset shows the guided modes in the k_x-k_y plane at a reduced frequency of 0.65. According to the scalability of Maxwell's equations, it is convenient to use a dimensionless frequency defined by $u=\frac{\omega a}{2\pi c}=\frac{a}{\lambda}$, with a some characteristic length of the system and λ the vacuum wavelength.

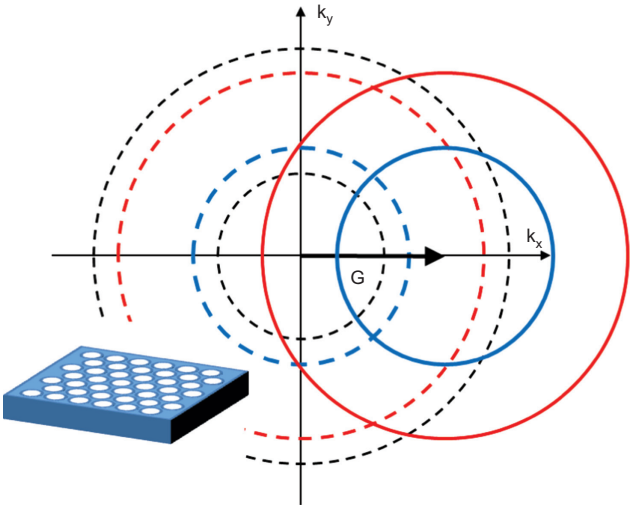

Figure 11 Bragg's diffraction of guided modes by reciprocal lattice vector **G** partially extracts guided modes. The inset shows the associated structure with a lattice constant a.

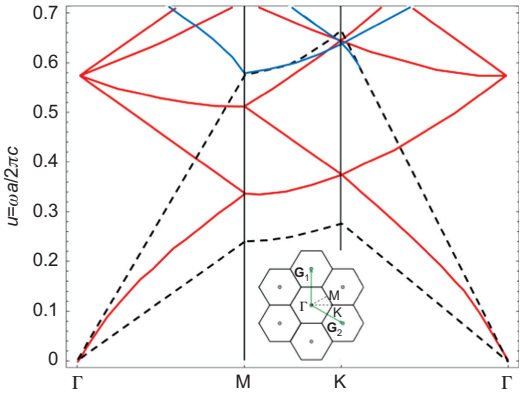

Figure 12 Dispersion relation of a periodically structured slab as shown in the inset of Figure 11 for negligible refractive index difference between holes and slab. Γ, M, and K are the main directions determining the Brillouin zone as depicted in the inset. The reciprocal lattice vectors $\mathbf{G}_1$ and $\mathbf{G}_2$ have length $G=\frac{4\pi}{\sqrt{3}a}$.

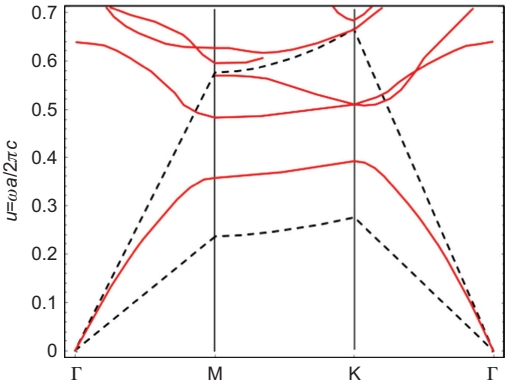

Figure 13 Dispersion relation of an etched through hexagonal photonic crystal in the slab of Figure 10 with a complete band gap for $0.4<u<0.48$.

are supported by a random structure and its corresponding Fourier transform. However, this does not violate the Second Law because besides diffraction into air other diffraction processes result in guided modes and not all the light is squeezed into the small vessel.

At the Brillouin zone edges of the regular photonic crystal structure, for example, at the M or K point, the modes are degenerate. Both states have the same in-plane k-vector but differ in the positioning of the mode profile relative to the lattice. Hence, the two states see different average refractive indices and consequently the degeneracy is lifted. In [7] the frequency shift is approximated by:

$$\frac{\Delta\omega}{\omega}=-\frac{\Delta n}{n}\cdot\left(\int_{structuring} n^2|E|^2\right). \quad (6)$$

Consequently, a large band-gap arises if the index contrast defining the photonic crystal is large and the photonic crystal covers a large fraction of the mode profile. If this is not the case, the frequency shift can be neglected and the photonic crystal acts as a pure diffraction grating.

Drilling air holes through the slab of Figure 10 gives the dispersion relation as shown in Figure 13. Owing to the large index contrast between air and slab material (n=2.4) a complete band-gap opens up.

By adjusting the emission wavelength to the band-gap of such a photonic crystal, it is possible to suppress emission into guided modes completely. Thus, only light is generated with $0<k_{||}<k_0$ and 100% extraction efficiency is possible. However, the efficiency of light generation itself gets worse in the presence of a band-gap according to Fermi's Golden Rule because the number of possible final states is heavily reduced [8], that is, the Purcell Factor drops [9] as only the modes with $0<k_{||}<k_0$ contribute as final states to the radiative electron-hole-recombination process. Guided modes that would occupy a much larger area in **k**-space are not present.

Alternatively, if the pitch is chosen in such a way that the emission takes place at the flat bands of the dispersion relation, for example, $u\approx0.7$, high extraction efficiencies and increased radiative recombination rates can be achieved [10]. The high radiative recombination rates stem from the high density of photonic states that come with flat bands. Nevertheless, etching through the whole layer stack of an LED implies a loss of light generating area equal to the area of holes that first has to be compensated before achieving a positive net effect.

An LED structure that overcomes this problem is presented in [11] where the photonic crystal is not etched

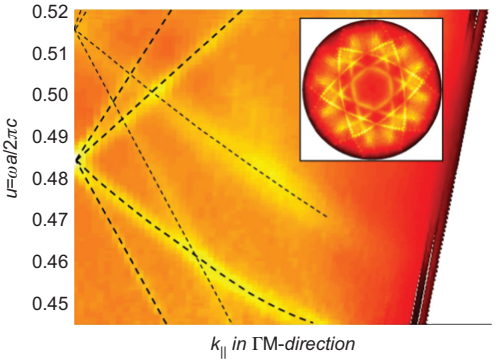

Figure 14 Measured dispersion relation of an LED structure from [11]. Dashed lines indicate calculated dispersion of the guided modes taking into account only the diffraction of modes while neglecting band-bending. The inset shows the k_x-k_y measurement at one frequency. The Star-of-David-shaped profiles stems from the diffraction of guided modes by the six reciprocal lattice vectors of a hexagonal lattice according to the geometrical construction of Figure 11.

through the active area but to almost 50% through an 850-nm thick LED cavity (Figure 14). Measurements of the dispersion relation above the light line [12] show good agreement with a calculation of the band diagram according to Bragg's law of diffraction as shown in Figure 12, that is, no strong band-bending occurs. For more details on photonic crystal LEDs, the reader is referred to [13] and [14] and references therein.

In general, with photonic crystals remarkable extraction efficiencies have been achieved especially if the LED layer design is optimized for the interaction with the structuring. Record efficiencies of up to 73% in air have been reported [15]. However, to date their design is not mass producible due to their thin overall thickness and the incorporated transparent contacts that introduce additional losses. Furthermore, state-of-the-art commercial devices are a tough benchmark with extraction efficiencies of up to 80% for InGaN [16, 17] and 50% for InGaAlP [18] with encapsulation realized by efficient recycling mechanisms.

4 Conclusion

When electric energy with zero entropy is converted to photons in an LED, it is the random distribution of those photons into the modes of the electromagnetic field within the LED which generates entropy. Thermodynamic considerations show that full direct extraction is then impossible, forbidden by the Second Law. For the LEDs with planar junctions which dominate the market today, rough surface structures and highly efficient recycling mechanisms within the chip, and to a certain extent also photonic crystals, can (and do) increase the out-coupling efficiency. However, to overcome the thermodynamic limitations on efficiency in a more fundamental way, it will be necessary to learn to control which modes are filled with photons in the first place.

Received May 22, 2013; accepted July 3, 2013

References

[1] E. F. Schubert, in 'Light-emitting Diodes' (Cambridge University Press, New York, 2006).
[2] H. Ries, A. Segal and J. Karni, Appl. Optics 36, 2869–2874 (1997).
[3] R. Winston, J. C. Minano and P. Benitez, in 'Nonimaging Optics' (Elsevier Academic Press, Burlington, MA, 2005).
[4] J. Muschaweck and H. Ries, Proc. SPIE 5942, 1–7 (2005).
[5] G. Kirchhoff, Ann. Phys. Chem. 109, 275–301 (1860).
[6] H. Benisty, H. de Neve and C. Weisbuch, IEEE J. Quant. Electron. 34, 1612–1631 (1998).
[7] J. Joannopoulos, S. Johnson, J. Win and R. Meade, in 'Photonic Crystals – Molding the Flow of Light' (Princeton University Press, Princeton, NJ, 2008).
[8] M. Fujita, S. Takahashi, Y. Tanaka, T. Asano and S. Noda, Science 308, 1296–1298 (2005).
[9] E. Purcell, Phys. Rev. 69, 681 (1946).
[10] M. Boroditsky, R. Vrijen, T. Krauss, R. Coccioli, R. Bhat, et al. J. Lightwave Technol. 17, 2096 (1999).
[11] K. Bergenek, C. Wiesmann, H. Zull, C. Rumbolz, R. Wirth, et al. IEEE J. Quant. Electron. 45, 1517–1523 (2009).
[12] A. David, C. Meier, R. Sharma, F. Diana, S. Den-Baars, et al. Appl. Phys. Lett. 87, 101107 (2005).
[13] C. Wiesmann, K. Bergenek, N. Linder and U. T. Schwarz, Laser Photon. Rev. 3, 262–286 (2009).
[14] A. David, H. Benisty and C. Weisbuch, Rep. Prog. Phys. 75, 12651 (2012).
[15] J. J. Wierer, D. Aurelien and M. M. Mischa, Nature Phot. 3, 163–169 (2009).
[16] V. Haerle, B. Hahn, S. Kaiser, A. Weimar, S. Bader, et al. Phys. Stat. Sol. (A) 201, 2736 (2004).
[17] M. Krames, O. Shchekin, R. Mueller-Mach, G. Mueller, L. Zhou, et al. J. Display Technol. 3, 160 (2007).
[18] R. Windisch, R. Butendeich, S. Illek, S. Kugler, R. Wirth, et al. IEEE Photon. Technol. Lett. 19, 774 (2007).

Julius Muschaweck is Senior Principal Key Expert for Optical Design at OSRAM GmbH. After studying physics at the University of Munich, Germany, he was co-founder and CEO of an engineering service company specializing in optical design for illumination. Since 2006, he works at OSRAM GmbH, where he is now the head of the Optical Technologies group at central R&D, and also the global coordinator of the optical design community within OSRAM. His expertise lies in the application of the theory of Nonimaging Optics to create efficient and affordable illumination optics for solid state lighting devices. He is also teaching illumination optics courses within OSRAM, for other industry customers, and at several universities.

Christopher Wiesmann works for OSRAM GmbH since 2005. He started with a PhD thesis on “Nano-structured LEDs – Light Extraction Mechanisms and Applications” mainly focusing on the application of photonic crystals for LEDs. Currently, he is with the Optical Technologies Group at Central R&D and his main research topics are non-imaging optics, light conversion and light extraction.